A complete ensemble empirical mode decomposition with adaptive noise deep autoregressive recurrent neural network method for the whole life remaining useful life prediction of lithium-ion batteries.

ZHANG, C., WANG, S., YU, C., WANG, Y. and FERNANDEZ, C.

2023

A complete ensemble empirical mode decomposition with adaptive noise deep autoregressive recurrent neural network method for the whole life remaining useful life prediction of lithium-ion batteries

Chuyan Zhang[1] · Shunli Wang[1,2] · Chunmei Yu[1] · Yangtao Wang[1] · Carlos Fernandez[3]

[1]   School of Information Engineering, Southwest University of Science and Technology, Mianyang 621010, China

[2]   College of Electrical Engineering, Sichuan University, Chengdu 610065, China

[3]   School of Pharmacy and Life Sciences, Robert Gordon University, Aberdeen AB10 7GJ, UK

Corresponding author: Shunli Wang wangshunli1985@qq.com

Abstract

The real-time prediction of the remaining useful life (RUL) of lithium-ion batteries provides an effective mean of preventing accidents. An improved adaptive noise-reduction deep learning method is applied to achieve adaptive noise-reduction decomposition of lithium-ion battery capacity using complete ensemble empirical mode decomposition with adaptive noise (CEEMDAN), and then the resulting intrinsic mode function (IMF) components are continued to be reconstructed, followed by input to a deep autoregressive recurrent neural network (DeepAR) to accurately predict the remaining useful life of lithium-ion batteries. To begin with, the lithium-ion battery data are screened and the correlation with capacity is analyzed by Pearson and Spearman to derive the indirect health factors. Then, the capacity data are decomposed by CEEMDAN to derive a relatively smooth IMF with the trend component for reconstruction, which is the output of the DeepAR model to predict the RUL of lithium-ion batteries with the indirect health factor as the output. The experimental results obtained after validation of the data set validate that the improved adaptive noise reduction DeepAR prediction model has superior prediction accuracy and greater stability, with all remaining life errors less than 5 times and all root mean square errors (RMSE) less than 2.5%.

Keywords Lithium-ion batteries, Remaining useful life, Health factor, Complete ensemble empirical mode decomposition with adaptive noise, Deep autoregressive recurrent neural network

Introduction

With the worldwide economy and the quick progress of new energy sources, as the optimal batteries for present energy storage, lithium-ion batteries have been the center of attention for a long time [1]. The lightweight, superior energy density, long cycle lifespan, broad operating temperature scope, and low cost are all merits of lithium-ion batteries [2, 3]. Lithium-ion batteries play a vital role as a core energy storage component in electric vehicles [4], aerospace systems [5], and other applications. Across various countries, renewable energy has drawn attention as an alternative to traditional fossil fuels [6]. Lithium-ion batteries are broadly applied and promoted in the field of renewable energy with the merits of high energy density, good output capacity [7], and cost effectiveness [8]. The development of this technology has provided new approaches to the development of high-performance electric vehicles and also to the development of electric vehicles [9]. However, the risk of battery combustion and fire still exists [10].

It is overt that the safety management system of the battery [11] should not be ignored. The remaining useful life (RUL) of lithium-ion batteries serves as a vital parameter [12] for users to grasp the aging status of the batteries at all times [13]. In the light of the current research progress, the prediction approaches of RUL can be broadly classified into two types, which are model-based and data-driven approaches [14, 15]. Liu et al. [16] presented a particle filtering framework based on an electrochemical model for capacity decline estimation of lithium-ion batteries. Zhang et al. [17] applied a double exponential

empirical model to the state model by using an extended Kalman particle filter algorithm to predict the RUL of lithium batteries. Huang et al. [18] chose an unscented Kalman filter algorithm that can efficiently resolve nonlinear issues for good prediction the RUL. The accuracy of the prediction of the remaining useful life of lithium-ion batteries is not optimal due to its own exceptionally complex internal chemistry, which can be evaluated by building models, while data-driven approaches can attain high-precision prediction [19, 20]. The current data-driven approach is more prevalent when it comes to neural network algorithms for prognosis [21, 22]. Lianbing et al. [23] employed differential voltage-Elman neural network for lithium-ion batteries. Other data-driven approaches have achieved superior and desirable results for the remaining useful life of lithium-ion batteries. Qiu et al. [24] proposed a new approach for remaining life estimation, which exploits the aging factor during charging and combines it with a multicore correlation vector machine. Chen et al. [25] suggested a novel approach based on empirical models and improved least squares support vector machines (LS-SVM) to successfully construct a RUL prediction framework. Chen et al. [26] presented an approach to estimate the RUL of lithium-ion batteries based on a combined model of two-phase Wiener and an extreme learning machine (ELM). A fundamental prerequisite for precise prediction of the lifetime of lithium batteries is the extraction of their highly correlated health characteristics [27].

It is clear from recent research results that many researchers have combined empirical mode decomposition (EMD) with data-driven methods to predict the RUL of lithium-ion batteries [28]. Liu et al. [29] decomposed the capacity data of lithium batteries using EMD and applied a combined long short-term memory (LSTM) and gaussian process regression (GPR) model to predict the battery RUL. Qinfeng et al. [30] decomposed the battery health factor and capacity data by EMD, and presented an empirical modal decomposition based on gravity search algorithm (GSA) fused with an ELM method for remaining life prediction of lithium batteries. The drawbacks of EMD algorithm include the standard demarcation of mode aliasing and stopping iteration in intrinsic modal function (IMF) decomposition [31]. Mao et al. [32] performed ensemble empirical mode decomposition (EEMD) of lithium battery data to obtain low-frequency and high-frequency data. The Gaussian or sine function Levenberg-Marquardt algorithm (GS-LM) was used to predict the low-frequency data, and the long short-term memory-sliding time window (LSTM-STW) algorithm was used to predict the high-frequency data. Yang et al. [33] inte- grated EEMD with gray wolf optimization-support vector regression (GWO-SVR) to establish a novel method that can be used to forecast the remaining life of Li-ion batteries. While the EEMD algorithm addresses the issue of modal confusion, the white noise generated by the decomposition process [34] and the reliance on empirical selection of IMFs still affect the precision of the decomposition [35]. EEMD is to add white noise to the primordial signal to alter the extreme point distribution of the signal [36], and CEEMD is to add a set of noise signals to the primordial signal to alter the extreme point distribution of the signal [37]. CEEMD gains calculation time by guaranteeing small residual noise interference [38]. Sun et al. [39] presented a new trace-free particle filtering algorithm developed using an optimal multiple kernel relevance vector machine (OMKRVM), and a CEEMD reconstruction algorithm is applied for noise reduction and estimation of the health status and remaining lifetime of Li-ion batteries. In Lyu et al. [40], the battery aging characteristics are decomposed into high-frequency and low-frequency components by CEEMD; then, LSTM neural network modeling and prediction are used for SOH estimation, and the GWO-based multi kernel relevance vector machine (MKRVM) is applied to RUL prediction. The components are decomposed by CEEMDAN to form the first-order intrinsic mode components, and immediately after ensemble averaging [41], which avoids the issue that the inconsistency of the IMF decomposition results of each group in CEEMD makes it hard to align the final set on average [42], it also avoids the subsequent decomposition when the decomposition of one of the orders of IMF is not good [43]. Qu et al. [44] suggested the IMF is proposed to be denoised using the complete ensemble empirical mode decomposition with adaptive noise (CEEMDAN) technique based on wavelet transform, and the IMF is trained, predicted, and reconstructed by least square-RVM using it as the input component. For the moment, a large amount of researchers adopt stochastic process to fit the battery degradation process [45]. A number of researchers employed health factors in this aspect to estimate the remaining useful life of lithium-ion batteries [46, 47].

The achievements of the above researchers largely cover adaptive noise reduction of battery data and using data-driven algorithms for prediction, while the data-driven approach has high requirements on the quality of the original data, and the trend of battery capacity degradation has a slight noise component which affects the precision of battery prediction. DeepAR is based on LSTM-RNN, but the architecture of this method is computationally more complex than other similar time series forecasting algorithms, and can make more accurate predictions of undulating and complex data outputs such as datasets of lithium-ion battery capacity. The proposed adaptive noise reduction approach decomposes the battery capacity by CEEMDAN, and the decomposed IMF components are reconstructed again, which will be used as the input data of DeepAR neural network to predict the RUL of lithium-ion batteries.

Theoretical analysis

CEEMDAN-DeepAR model

The flow chart of the proposed method to forecast the RUL of lithium-ion batteries is shown in Fig. 1. The major steps are described below:

(1) Capacity voltage and current data are extracted from the NASA dataset and health features are extracted from them, and then correlation analysis is performed.

(2) The strongly correlated indirect health factors are screened out as the input to the model.

(3) Adaptive noise reduction decomposition is performed on the capacity data of lithium-ion batteries using CEEMDAN to obtain IMF components.

(4) The obtained IMFs are reconstructed and then input into the incoming DeepAR model for training and pre- diction.

(5) Finally, the predicted results are evaluated in various aspects to test the precision of the presented algorithm.
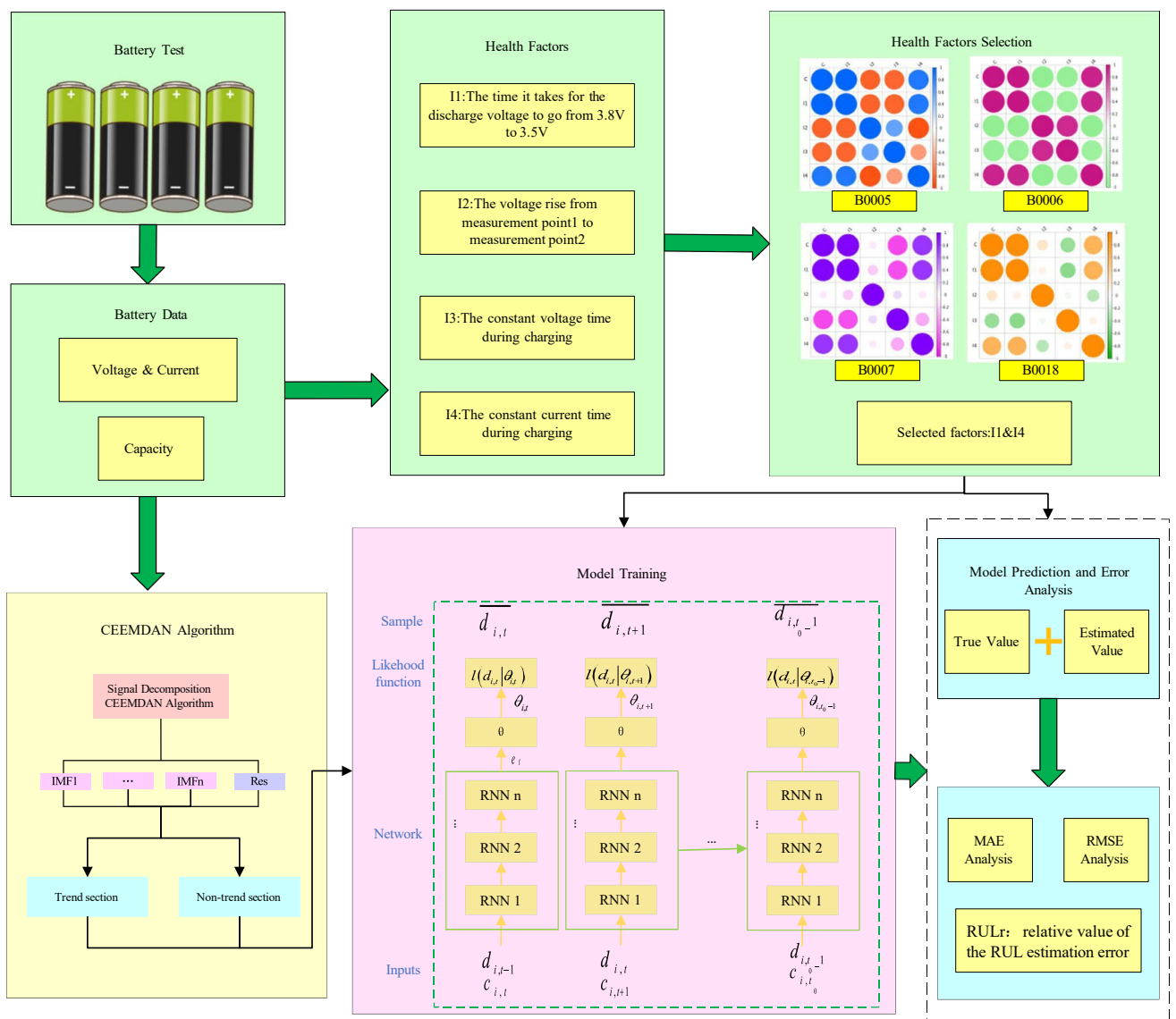

Fig. 1 The CEEMDAN-DeepAR model structure

CEEMDAN algorithm

A superior noise reduction algorithm is derived from the EMD and EEMD algorithms through continuous enhancement of CEEMDAN. No pre-processing and analysis are applied in this algorithm for signal decomposition. However, there are multiple eigenmode functions (IMFs) and multiple residuals (R) in the time series, and these eigenvalues can be decomposed adaptively. The approaches have been broadly used in predictive models of nonlinear and non-smooth signals and time series. CEEMDAN overcomes the frequent modal mixing issue of the EMD algorithm [48] and resolves the problem that the EEMD algorithm cannot remove the added white noise, resulting in incomplete decomposition and wide reconstruction errors [49]. The decomposition process was refined and the CEEMDAN method was proposed by Torres et al. [50]. It controls the noise level by introducing a white noise signal- to-noise ratio (SNR) attached to every decomposition process.

The Gaussian white noise is inserted into the signal to be decomposed to gain a new signal:

$$\hat{g}_t = g(t) + (-1)^q \varepsilon v^j(t) \tag{1}$$

The individual components in Eq. (1) are presented as follows: $g(t)$ represents the signal to be decomposed, ε rep- resents the variance of the noise, and v^j represents the Gaussian white noise with zero unit variance.

The total average of the derived N modal components yields the IMF1 of the CEEMDAN decomposition:

$$\overline{I_i(t)} = \frac{1}{N} \sum_{j=1}^{N} I_1^j(t) \tag{2}$$

The individual components in Eq. (2) are presented as follows: $\overline{I_i(t)}$ represents the ith eigenmode component obtained by CEEMDAN decomposition. The residual signal at this point becomes:

$$R_1(t) = g(t) - \overline{I_1(t)} \tag{3}$$

Add positive and negative paired Gaussian white noise to $R_1(t)$ and decompose it to derive the first-order modal component D_1, which yields the new signal. This provides the second eigenmodal component of the CEEMDAN decomposition:

$$\overline{I_2(t)} = \frac{1}{N} \sum_{j=1}^{N} D_1^j(t) \tag{4}$$

The 2nd residual signal is expressed as:

$$R_2(t) = R_1(t) - \overline{I_2(t)} \tag{5}$$

Repeat the above steps until the decomposition condition of EMD cannot be satisfied by the remaining residual signal. Eventually, the original signal is decomposed as follows:

$$g(t) = \sum_{k=1}^{K} \overline{I_k(t)} + R_k(t) \tag{6}$$

DeepAR algorithm

A probabilistic forecast approach based on auto-regressive recurrent neural networks called DeepAR [51]. The approach addresses the prediction issue through deep neural network learning, combined with appropriate likelihoods, using nonlinear data transformation techniques [52]. Traditionally, time series forecasting faces challenges related to data, such as the failure to obtain complete data on all influencing factors and the uncertainty of influencing factors in the future [53].

DeepAR relieves the data requirements to a certain extent. As a supervised learning algorithm, DeepAR adds default values directly inside the model [54]. In the process of importing data, there is no requirement to artificially scan the data for default values; DeepAR models address this issue internally [55]. By using DeepAR, time series can be correlated with multiple groupings; non-linear issues and scale issues that are hard to handle statistically can be handled. In the application of lithium-ion battery aging prediction, when strong correlations of historical data affecting lithium-ion battery aging are input, the future aging trend of the battery can be predicted, and the remaining useful life of the lithium-ion battery can be readily known when the battery is used.

The time series of DeepAR model is defined as $d_{i,t}$, and t_0 is considered the interval time node between the training process and the prediction process. By modeling the time series data with the training process range $[1, t_0 - 1]$ and the covariate $c_{i,t}$ and training them using the likelihood form of Eq. (7):

$$Q_\theta\left(d_{i,t_0:T}\middle|d_{i,1:t_0-1}, c_{i,1:T}\right) = \prod_{t=t_0}^{T}\ell\left(d_{i,t}\middle|\theta\left(e_{i,t}, \theta\right)\right) \qquad (7)$$

In Eq. (7) where $e_{i,t} = e(e_{i,t-1}, d_{i,t-1}, c_{i,t}, \theta)$ is the output of the autoregressive recurrent network. $e(\cdot)$ represents an RNN, inputs the hidden layer $e_{i,t-1}$ of the last moment and the data $d_{i,t-1}$, and the known information $c_{i,t}$ of the current moment to derive the hidden layer $e_{i,t}$ of that moment (i.e., the output), and then transform $e_{i,t-1}$ into the parameters of the given distribution through the neural network $\theta(\cdot)$. After the distribution is determined, the likelihood can be calculated $\ell(d_{i,t}|\theta(e_{i,t}, \theta))$.

Fig. 2 depicts the overall process of DeepAR algorithm. For the training process, where all data are known, the prediction range data are directly input, and then the likelihood function is calculated for the next moment, and the model parameters are trained by maximizing the likelihood function. For the prediction process, the data of the prediction range is unknown, and only an estimated value can be derived by sampling, and input the estimated value into the RNN at the next time, in order to achieve the prediction results by iterating continuously.
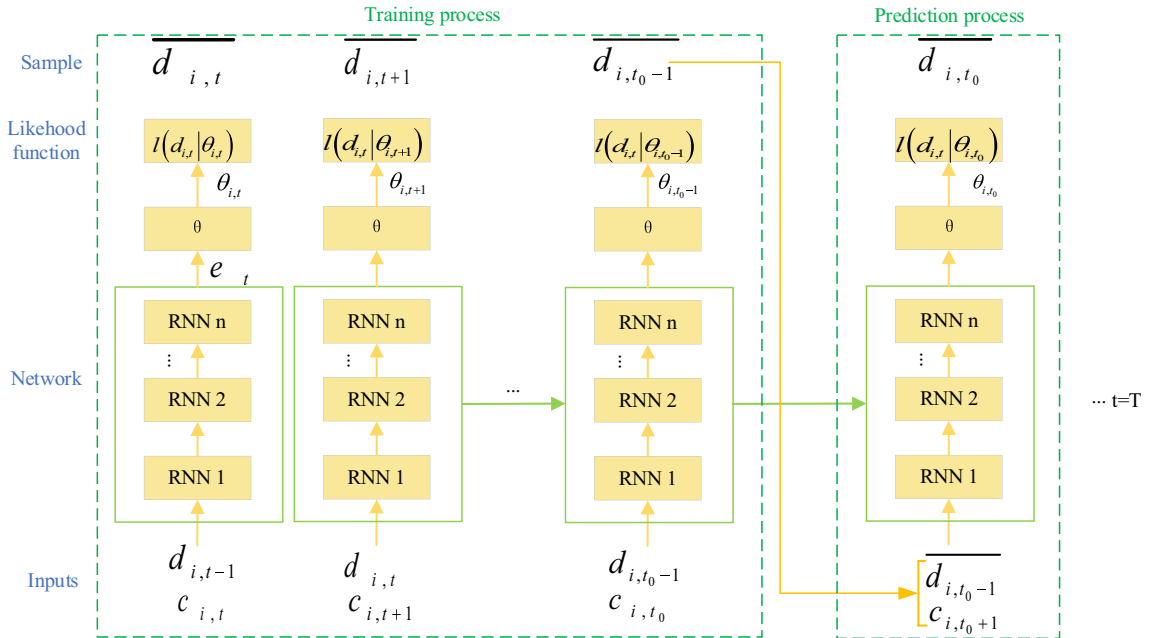

Fig. 2 Flowchart of DeepAR algorithm

Indirect health factor extraction

Construction of indirect health factors

Based primarily on the aging trend of lithium-ion batteries, the remaining useful life of the battery is predicted by health factors. There are direct and indirect health factors; the distinction between them is that direct health factors such as discharge capacity are directly relevant to the remaining useful life of the battery; nevertheless, indirect health factors are health factors that are highly correlated with the discharge capacity of Li-ion batteries, for example, the currently known equal voltage drop discharge time.

A relevant mathematical model has been developed to predict the remaining service life of Li-ion batteries using available capacity information and the number of cycles belongs to direct prediction, whereas indirect prediction which refers to the correlation model between non-direct health factors is established to carry out the study of the remaining service life of lithium-ion batteries, and the practical decay capacities. In comparison with the direct forecasting method, the indirect forecasting method is versatile and adaptable.

Indirect health factors

Fig. 3 reveals how the indirect health factors were extracted and screened in the following steps.

(1) Health factor extraction. Firstly, the voltage, time, and temperature of various stages of charging and discharging are extracted from the charging and discharging data of lithium-ion batteries from NASA dataset.

(2) Construction of indirect health factors. The extracted measured data are produced to generate truncated indirect health factors.

(3) Correlation analysis. For the correlation analysis between the various indirect health factors and the practical discharge capacity, the correlation coefficient is derived.

(4) Extraction of highly correlated indirect health factors. By comparing the correlation of each indirect health factor, the highly correlated indirect health factors are selected to serve as a strong basis for subsequent prediction.
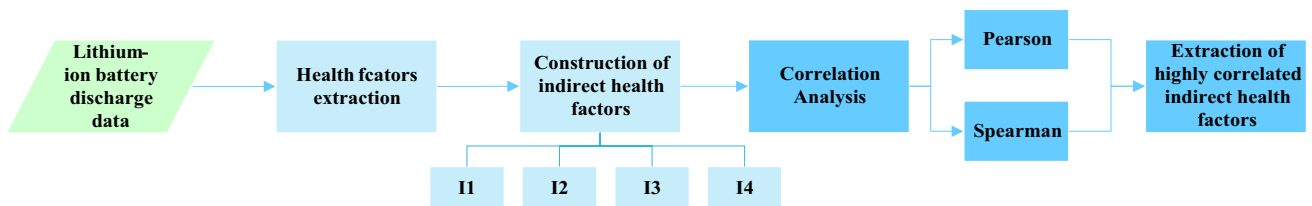

Fig. 3 Indirect health factors extraction framework

Correlation analysis

In the Pearson coefficient, which reveals the ratio of the quotient of the covariance of the two components to their standard deviation, it is denoted by p.

$$p_{XY} = \frac{\text{cov}(X, Y)}{\sigma_X \sigma_Y} = \frac{E(XY) - E(X)E(Y)}{\sqrt{E(X^2) - E^2(X)}\sqrt{E(Y^2) - E^2(Y)}} \quad (8)$$

In Eq. (8), $cov(X, Y)$ denotes the covariance of variables X and Y σ_X, σ_Y denote the standard deviation of variables X, Y; and E(X) denotes the mathematical expectation of X, and E(Y) denotes the mathematical expectation of Y.

Spearman is looking at X and Y as two sequences, and the focus is on whether the monotonicity of the two sequences is consistent.

$$p_s = 1 - \frac{6\sum_{i=1}^{n} d_i^2}{n(n^2 - 1)} \tag{9}$$

In Eq. (9), d_i denotes the difference of two variable levels. The more infinite the absolute value of the correlation coefficient, the greater the degree of correlation between the two variables.

Experimental analysis

Experimental data presentation

In this paper, NASA PCoe's published lithium-ion battery test data was adopted, which applied to a 18650 lithium-ion battery with 2 Ah capacity. In this study, three main steps are included: charging, discharging, and AC current impedance determination. In this research, B0005, B0006, B0007, and B0018 were used as the research objects. Battery pack testing completed at ambient temperature, in which the battery was charged at a steady current (CC) mode of 1.5A until the battery voltage reached 4.2V, followed by a steady voltage (CV) mode until the charging current was reduced to 20 mA. When the battery reached the disconnect voltage and ceased discharging, each charge and discharge was followed by a constant current (CC) of 2A discharge. The battery remains in a continuous accelerated aging cycle until the end of its useful life, when the maximum charge drops by 30%. The test conditions and recorded data for each cycle are indicated in Table 1 and Table *2*.

Table 1 Dataset battery pack experimental conditions

Battery	Temperature	Charging current	Discharging current	Cut-off voltage
B0005	24 °C	1.5A	2A	2.7V
B0006	24 °C	1.5A	2A	2.5
B0007	24 °C	1.5A	2A	2.2
B0018	24 °C	1.5A	2A	2.5

Table 2 Dataset experimental data

Charging process	Discharge process	Impedance measurement
Battery voltage	Battery voltage	Induction current
Battery current	Battery current	Battery current
Load voltage	Load voltage	Battery impedance
Load current	Load current	Calibration impedance
Time	Time	Ohmic resistance
–	Discharge power	Charge transfer impedance

Results and analysis

In this paper, CEEMDAN-DeepAR-based RUL estimation prediction is implemented using lithium-ion battery data. The proposed RUL model is input by applying indirect health factors with adaptive noise reduction integration of the actual battery capacity, as well as modeling and coaching on MATLAB2018a.

Indirect health factor extraction

For the purpose of accurate estimation of RUL of lithium-ion batteries, firstly, the indirect health factors of lithium-ion batteries are extracted, and the specific data are shown in Table 3.

Table 3 Lithium-ion battery health factor description

Factor	Factor description
I1	The time it takes for the discharge voltage to go from 3.8 to 3.5V
I2	The constant current time during charging
I3	The time to peak temperature
I4	The voltage rise from measurement point 1 to measurement point 2

Since each health factor has distinct tendencies, a direct evaluation of the relationship between them and capacity is not available. In this study, the relationship between health factors and actual capacity was quantitatively evaluated using Pearson and Spearman correlation coefficients.

In this paper, two indirect health factors with Pearson's coefficient and Spearman's coefficient larger than 0.75 are adopted as input parameters to guarantee that the extracted indirect health factors can cater for various circumstances. From Fig. 4 and Table 4, evidently, there is a close relationship between I1 and I4 and the true capacity; thus, it is a practical approach to use the voltage drop time and charge/discharge cycle with the charge/discharge cycle from the first charge to the first charge, and the charge/discharge cycle, respectively, as the health factors that indirectly affect the remaining battery life.

Table 4 The correlation coefficients of HFs

Battery	Correlation analysis	I1	I2	I3	I4
B0005	Pearson	0.9972	−0.8354	−0.8185	0.8777
	Spearman	0.9983	−0.8233	−0.8343	0.8825
B0006	Pearson	0.9969	−0.9061	−0.9113	0.9394
	Spearman	0.9995	−0.9129	−0.9043	0.9477
B0007	Pearson	0.9788	−0.0977	−0.7381	0.7849
	Spearman	0.9872	−0.0935	−0.7175	0.7902
B0018	Pearson	0.9713	−0.2067	−0.4286	0.7790
	Spearman	0.9826	−0.2116	−0.4325	0.7960

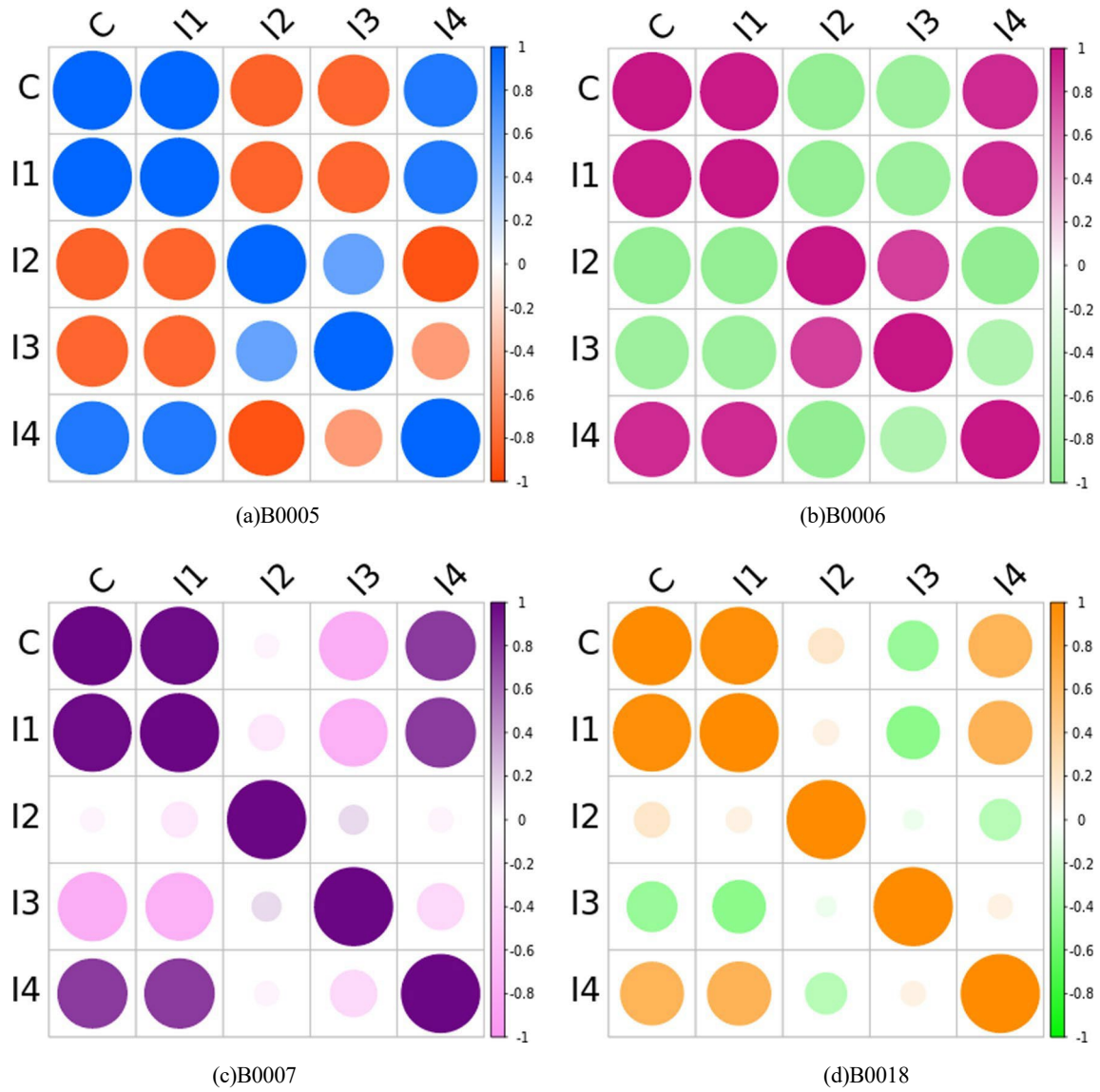(a)B0005   (b)B0006

(c)B0007   (d)B0018

Fig. 4 Correlation analysis chart for health factors by using Pearson

The analysis of RUL prediction results

The data adopted in this study were firstly decomposed by adaptive noise reduction to derive the noise reduction data, and then the acquired indirect health factors and the noise reduction capacity data were trained with the DeepAR model followed by the RUL prediction of the battery. In order to visualize the prediction accuracy of the algorithm more intuitively, the mean absolute error (MAE) and root mean square error (RMSE) are used to evaluate the behavior of the method.

$$RMSE = \sqrt{\frac{1}{N}\left(\sum_{i=1}^{N}\left(x_i - \hat{x}_i\right)^2\right)} \tag{10}$$

$$MAE = \frac{1}{N}\sum_{i=1}^{N}\left|x_i - \hat{x}_i\right| \tag{11}$$

3.1.1.1 Results of CEEMDAN decomposition

The amount of noise added is 50 and the signal-to-noise ratio (SNR) is 0.0005. The capacity decomposition results for B0005, B0006, B0007, and B0018 are plotted in Fig. 5 where it can be noticed that noise signals due to capacity regeneration can be seen in each curve. These interferences can lead to changes in the capacity curves, which can adversely affect the subsequent capacity prediction. IMF1 can indicate the primary trend degradation, the capacity recovery path of IMF2, and unknown interference and noise trends for IMF3, 4, 5 and IMF6. This serves as a guide for CEEMDAN in reducing the sophistication of the model.

(B0005)

(B0006)

(B0007)

(B0018)
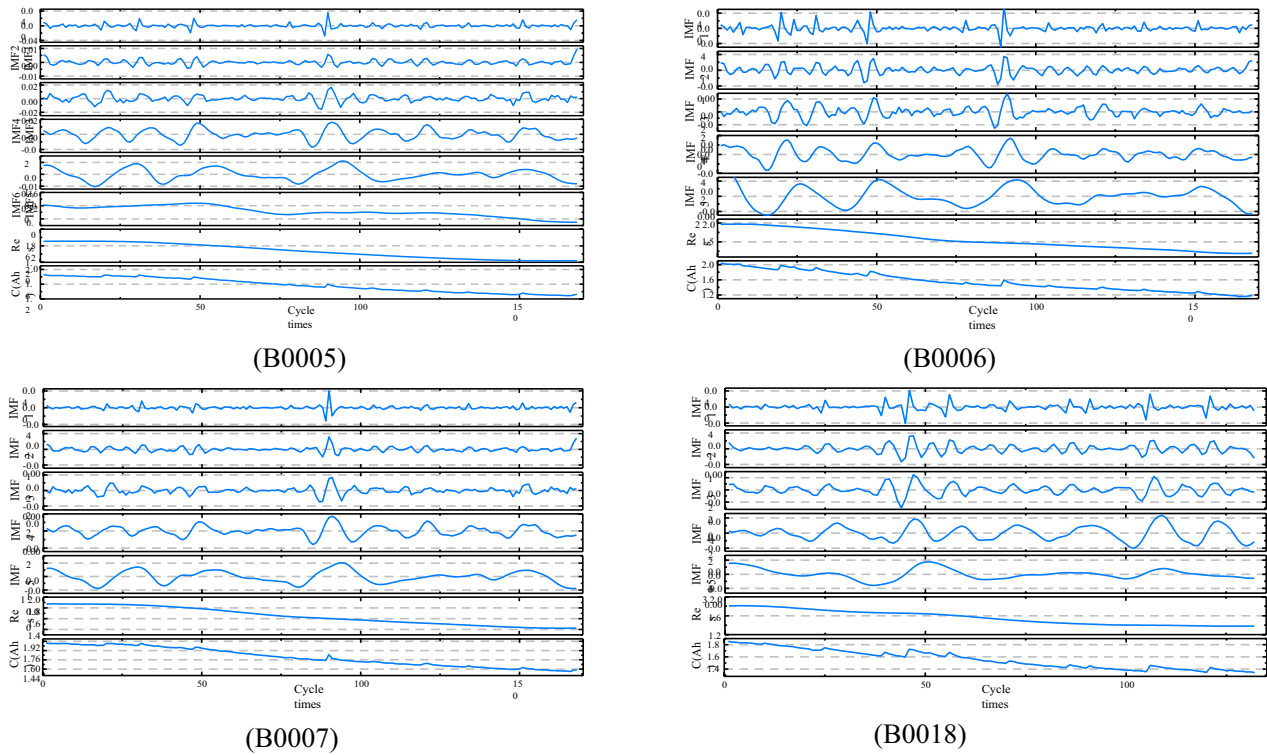
Fig. 5 Capacity decomposition results

3.1.1.2 Results of RUL estimation

The objective of this paper aims to verify that the capacity data after adaptive noise reduction can more closely match the degradation trend of lithium-ion batteries themselves to attain the goal of precise RUL prediction. For B0005 and B0007, the former 69 data are categorized as the training set and the rest as the test set, and for B0006and B0018, the former 49 data are categorized as the training set and the remaining backup as the test set. After the prediction of battery RUL by DeepAR model, the results and error diagram are shown below. It is apparent that the prediction results without adaptive noise reduction have a large error fluctuation, while the prediction results of the method proposed in this paper can conform to the actual capacity degradation trend well.

As in Table 5, RULp stands for the RUL prediction of the battery; RULt stands for the practical RUL value; the above mentioned indexes are in units of: times; RULe represents the absolute value of the RUL estimation error, which is defined in Eq. (12); RULr represents the relative value of the RUL estimation error, showed in Eq. (13):

Table 5 Comparison of the RUL prediction performance

	Algorithm	RUL_p	RUL_t	RUL_e	RUL_r
B0005	DeepAR	67	63	4	6.35%
	CEEMDAN-DeepAR	64		1	1.59%
B0006	DeepAR	102	108	6	5.56%
	CEEMDAN-DeepAR	107		1	0.93%
B0007	DeepAR	44	51	7	13.73%
	CEEMDAN-DeepAR	46		5	9.80%
B0018	DeepAR	50	57	7	12.28%
	CEEMDAN-DeepAR	53		4	7.02%

$$RUL_e = \left| RUL_p - RUL_t \right| \tag{12}$$

$$RUL_r = \frac{\left| RUL_p - RUL_t \right|}{RUL_t} \times 100\% \tag{13}$$

From Fig. 6 and Table 5, compared with using just the DeepAR algorithm, the life prediction performance of the four groups of lithium-ion batteries after noise reduction by the CEEMDAN algorithm and then input into the DeepAR model is superior, and the prediction curve is similar to the practical capacity decay curve; the prediction error of the CEEMDANN-DeepAR model is minimum at 1 cycle. Since it can better reflect the performance change law of lithium-ion battery, the model can better reflect the performance change law of lithium-ion battery. To better display the prediction accuracy of this study, the RMSE and MAE will be used to evaluate the results (Table 6).

Table 6 RUL estimation error results

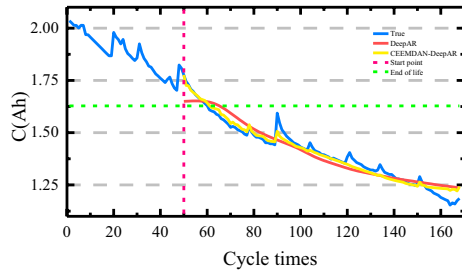| Battery	Algorithm	MAE	RMSE
B0005	DeepAR	0.0101	0.0142
	CEEMDAN-DeepAR	0.0063	0.0097
B0006	DeepAR	0.0359	0.0432
	CEEMDAN-DeepAR	0.0193	0.0258
B0007	DeepAR	0.0161	0.0231
	CEEMDAN-DeepAR	0.0103	0.0125
B0018	DeepAR	0.0400	0.0522
	CEEMDAN-DeepAR	0.0169	0.0226

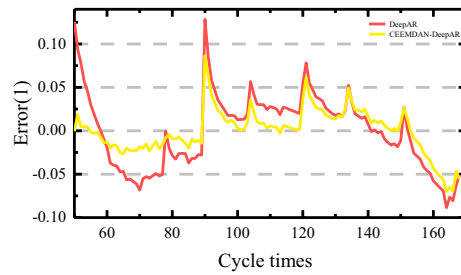**Fig. 6** Results of RUL estimation (start point=50/70)
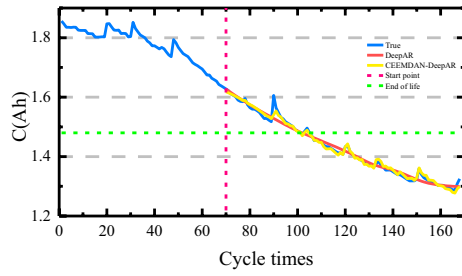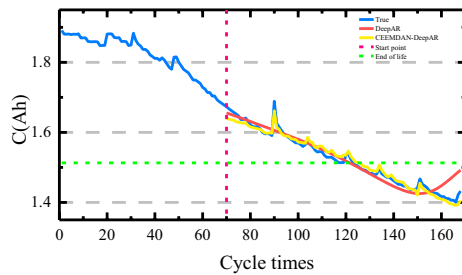

(a) B0005 comparison of predicted trends
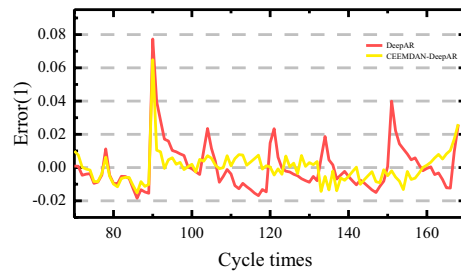
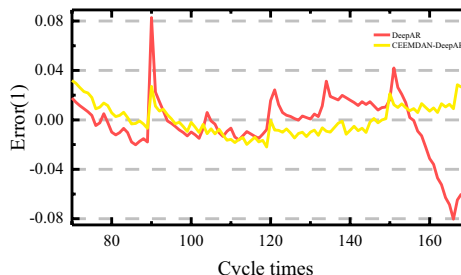(b) B0005 comparison of prediction errors
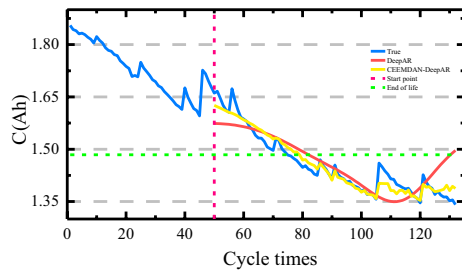
(c) B0006 comparison of predicted trends

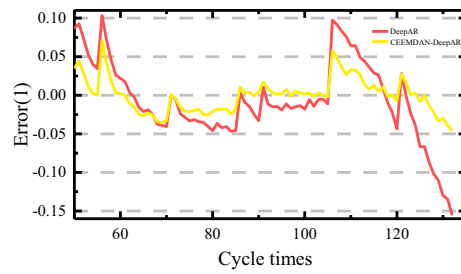(d) B0006 comparison of prediction errors

(e) B0007 comparison of predicted trends

(f) B0007 comparison of prediction errors

(g) B0018 comparison of predicted trends

(h) B0018 comparison of prediction errors

It can be further observed from the prediction errors of RUL for the four batteries at decreasing prediction starting points presented in Table 7. It is readily apparent that the remaining life errors for all four batteries are within 10 times and decrease with increasing prediction starting point values when compared with Table 5. From this, it is apparent that the forecast error for the remaining useful life remains largely unchanged when the proposed model changes the prediction start point.

Table 7 Comparison of the RUL prediction performance

|	Algorithm	RUL_p	RUL_t	RUL_e	RUL_r
B0005	DeepAR	68	63	5	7.94%
	CEEMDAN-DeepAR	66		3	4.76%
B0006	DeepAR	111	108	3	2.78%
	CEEMDAN-DeepAR	107		1	0.93%
B0007	DeepAR	43	51	8	15.69%
	CEEMDAN-DeepAR	45		6	11.76%
B0018	DeepAR	52	57	5	8.77%
	CEEMDAN-DeepAR	58		1	1.75%

In Table 8, compared with the unoptimized DeepAR algorithm, the approach in this paper has a narrower forecasting precision, with a minimum MAE of 0.0063 and a minimum RMSE of 0.0097 for the CEEMDAN-DeepAR algorithm, which can attain the demand for prediction of the remaining life of lithium-ion batteries.

Table 8 RUL estimation error results

Battery	Algorithm	MAE	RMSE
B0005	DeepAR	0.0102	0.0148
	CEEMDAN-DeepAR	0.0046	0.0081
B0006	DeepAR	0.0414	0.0487
	CEEMDAN-DeepAR	0.0183	0.0230
B0007	DeepAR	0.0117	0.0176
	CEEMDAN-DeepAR	0.0085	0.0115
B0018	DeepAR	0.0285	0.0357
	CEEMDAN-DeepAR	0.0086	0.0122

The validation of the proposed model was carried out by designing different prediction starting points (the starting points were set to 70 for B0005, B0007 and 40 for B0006, B0018). Figure 7 illustrates that for the four lithium-ion batteries, the prediction curves keep similar degradation trends to the real data curve and fluctuate up and down around the real data under different prediction starting points as above. It is evident that no matter what prediction starting point is decided, there is no significant difference from the actual situation.
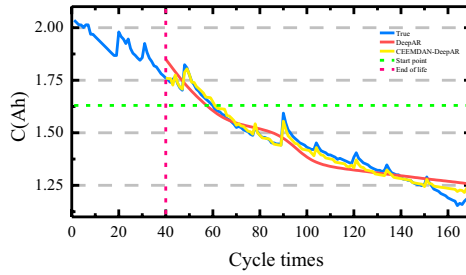
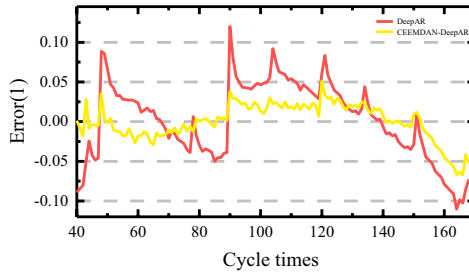**Fig. 7** Results of RUL estimation (start point=40/60)
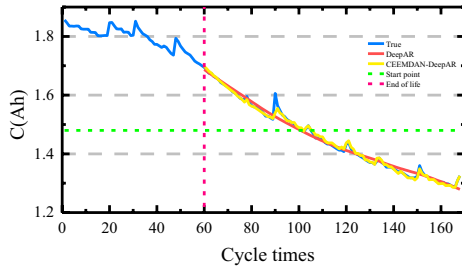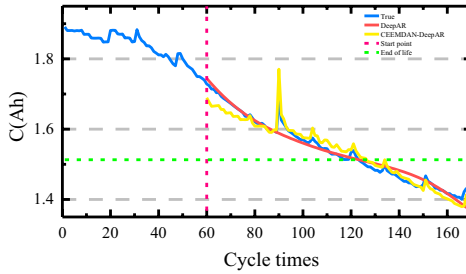

(a) B0005 comparison of predicted trends
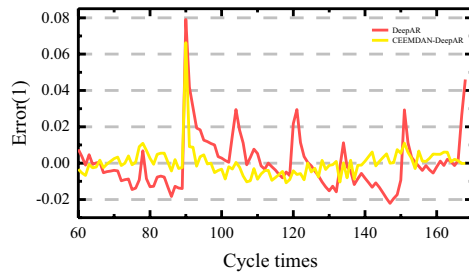
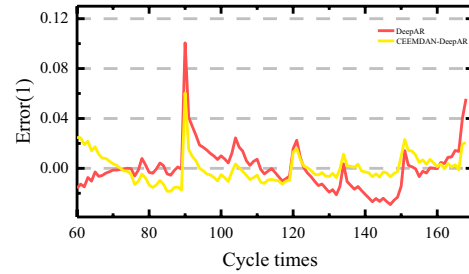(b) B0005 comparison of prediction errors
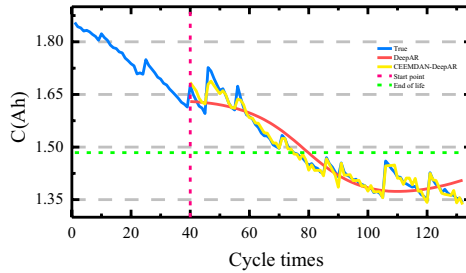
(c) B0006 comparison of predicted trends
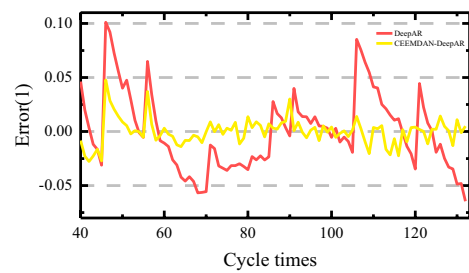
(d) B0006 comparison of prediction errors

(e) B0007 comparison of predicted trends

(f) B0007 comparison of prediction errors

(g) B0018 comparison of predicted trends

(h) B0018 comparison of prediction errors

The prediction errors of RUL for the four batteries at decreasing prediction starting points are presented in Table 7. It is readily apparent that the remaining life errors for all four batteries are within 10 times and decrease with increasing prediction starting point values when compared with Table 5. From this, it is apparent that the forecast error for the remaining useful life remains largely unchanged when the proposed model changes the prediction start point.

As can be further observed from Table 8, the decrease in the prediction starting point corresponds to a larger prediction error instead, and the proposed method has a narrower prediction accuracy compared with the unoptimized DeepAR algorithm, with a minimum MAE of 0.0046 and a minimum RMSE of 0.0081 for the CEEMDAN-DeepAR algorithm, which meets the requirements for predicting the remaining life of lithium batteries. It is clear that the RUL estimation algorithm has a high accuracy, and the reconstruction of the lithium battery capacity data after noise elimination by extracting the strong correlation of indirect health factors makes this greatly increase the estimation accuracy of the text and has more practical value.

Conclusion

In view of this, this paper intends to develop a novel method for predicting the remaining life of Li-ion batteries based on deep neural networks. Multiple variable information, such as voltage, temperature, and time, are extracted from the discharge/charge process. By using correlation coefficients, indirect health factors are filtered out and used as inputs to the CEEMDAN-DeepAR model, and the capacity data after CEEMDAN de-noising is used as the output. The model was validated using NASA lithium battery data, and tests indicated that the RUL estimation precision of the method was extremely high: the high accuracy of the proposed model RUL prediction is further demonstrated by different prediction starting points, and the maximum RMSE of the prediction is 0.0230. To further improve the safety and correctness of Li-ion batteries, this article has three areas for improvement: (1) the selection of more health indices to reflect the performance of Li-ion batteries; (2) the development of an electrochemical model of the battery; and (3) the implementation of a better algorithm for the parameter problem in this model.

Declarations

References

1. Yu X, Manthiram A (2021) Sustainable battery materials for next-generation electrical energy storage. Adv Sustain Syst 2(5):2000102
2. Wang Y, Wang E, Zhang X et al (2021) High-voltage "single-crystal" cathode materials for lithium-ion batteries. Energy Fuel 35(3):1918–1932
3. Che Y, Hu X, Lin X et al (2023) Health prognostics for lithium-ion batteries: mechanisms, methods, and prospects. Energy Environ Sci 16:338–371
4. Li Y, Yu L, Hu W et al (2020) Thermotolerant separators for safe lithium-ion batteries under extreme conditions. J Mater Chem A 8(39):20294–20317
5. Zhao L, Wang Y, Cheng J (2019) A hybrid method for remaining useful life estimation of lithium-ion battery with regeneration phenomena. Appl Sci 9(9):1890
6. Xiong HY, Liu H, Zhang RH et al (2019) An energy matching method for battery electric vehicle and hydrogen fuel cell vehicle based on source energy consumption rate. Int J Hydrog Energy 44(56):29733–29742
7. Che Y, Vilsen SB, Meng J et al (2023) Battery health prognostic with sensor-free differential temperature voltammetry reconstruction and capacity estimation based on multi-domain adaptation. Etransportation 17:100245
8. Zhang X, Han Y, Zhang W-P (2021) A review of factors affecting the lifespan of lithium-ion battery and its health estimation methods. Trans Electr Electron Mater 22(5):567–574
9. Geronikolos I, Potoglou D (2021) An exploration of electriccar mobility in Greece: a stakeholders' perspective. Case Stud Transp 9(2):906–912

10. Sripad S, Bills A, Viswanathan V (2021) A review of safety considerations for batteries in aircraft with electric propulsion. MRS Bull 46(5):435–442

11. Carkhuff BG, Demirev PA, Srinivasan R (2018) Impedance-based battery management system for safety monitoring of lithium-ion batteries. IEEE Trans Ind Electron 65(8):6497–6504

12. Jiang B, Dai H, Wei X et al (2021) Multi-kernel relevance vector machine with parameter optimization for cycling aging prediction of lithium-ion batteries. IEEE J Emerg Sel 11(1):175–186

13. Che Y, Stroe D-I, Hu X et al (2022) Semi-supervised self-learning-based lifetime prediction for batteries. IEEE Trans Industr Inform 19(5):6471–6481

14. Chen Z, Shi N, Ji Y et al (2021) Lithium-ion batteries remaining useful life prediction based on BLS-RVM. Energy 234:121269

15. Che Y, Deng Z, Lin X et al (2021) Predictive battery health management with transfer learning and online model correction. IEEE Trans Veh Technol 70(2):1269–1277

16. Liu Q, Zhang J, Li K et al (2020) The remaining useful life prediction by using electrochemical model in the particle filter framework for lithium-ion batteries. Ieee Access 8:126661–126670

17. Zhang N, Xu A, Wang K et al (2021) Remaining useful life prediction of lithium batteries based on extended kalman particle filter. IEEJ Trans Electr Electron Eng 16(2):206–214

18. Huang M, Zhang Q (2020) Prediction of remaining useful life of lithium-ion battery based on UKF; proceedings of the 2020 Chinese Automation Congress (CAC), F. IEEE

19. Wang R, Feng H (2021) Remaining useful life prediction of lithium-ion battery using a novel health indicator. Qual Reliab Eng Int 37(3):1232–1243

20. Mawonou KS, Eddahech A, Dumur D et al (2021) State-of-health estimators coupled to a random forest approach for lithium-ion battery aging factor ranking. J Power Sources 484:229154

21. Khumprom P, Yodo N (2019) A data-driven predictive prognostic model for lithium-ion batteries based on a deep learning algorithm. Energies 12(4):660

22. Che Y, Zheng Y, Wu Y et al (2022) Data efficient health prognostic for batteries based on sequential information-driven probabilistic neural network. Appl Energy 323:119663

23. Lianbing L, Sijia L, Jie L et al (2021) RUL prediction of lithium-ion battery based on differential voltage and Elman neural net-work. Energy Storage Sci and Techn 10(6):2373

24. Qiu JS, Fan YC, Wang SL et al (2022) Research on the remaining useful life prediction method of lithium-ion batteries based on aging feature extraction and multi-kernel relevance vector machine optimization model. Int J Energy Res 46(10):13931–13946

25. Chen W, Cai Y, Li A et al (2022) Remaining useful life prediction for lithium-ion batteries based on empirical model and improved least squares support vector machine; proceedings of the Proceedings of 2021 Chinese Intelligent Automation Conference, F. Springer

26. Chen X, Liu Z, Wang J et al (2021) An adaptive prediction model for the remaining life of an Li-ion battery based on the fusion of the two-phase wiener process and an extreme learning machine. Electronics 10(5):540

27. Tang T, Yuan H (2021) The capacity prediction of Li-ion batteries based on a new feature extraction technique and an improved extreme learning machine algorithm. J Power Sources 514:230572

28. Wang J, Zhang S, Li C et al (2022) A data-driven method with mode decomposition mechanism for remaining useful life pre-diction of lithium-ion batteries. IEEE Trans Power Electron 37(11):13684–13695

29. Liu K, Shang Y, Ouyang Q et al (2020) A data-driven approach with uncertainty quantification for predicting future capacities and remaining useful life of lithium-ion battery. IEEE Trans Ind Electron 68(4):3170–3180

30. Qinfeng Z, Yanping C, Xingjun W. Remaining useful life of Lithium-ion batteries based on EMD-GSA-ELM; proceedings of the 2021 IEEE 2nd International Conference on Information Technology, Big Data and Artificial Intelligence (ICIBA), F, 2021. IEEE.

31. Pająk M, Muślewski Ł, Landowski B et al (2019) Fuzzy identification of the reliability state of the mine detecting ship propulsion system. Pol Marit Res 26(1):55–64

32. Mao L, Xu J, Chen J et al (2020) A LSTM-STW and GS-LM fusion method for lithium-ion battery RUL prediction based on EEMD. Energies 13(9):2380

33. Yang Z, Wang Y, Kong C (2021) Remaining useful life prediction of lithium-ion batteries based on a mixture of ensemble empirical mode decomposition and GWO-SVR model. IEEE Trans Instrum Meas 70:1–11

34. Zhai H, Xiong W, Li F et al (2022) Prediction of cold rolling gas based on EEMD-LSTM deep learning technology. Assem Autom 42(2):181–189

35. Zheng J, Su M, Ying W et al (2021) Improved uniform phase empirical mode decomposition and its application in machinery fault diagnosis. Measurement 179:109425

36. Zhong C, Wang J-S, Sun W-Z (2022) Fault diagnosis method of rotating bearing based on improved ensemble empirical mode decomposition and deep belief network. Meas Sci Technol 33(8):085109

37. Li G, Ma S, Cai Y et al (2022) Application of CEEMD and per-mutation entropy in noise elimination of hydropower unit swing signal; proceedings of the Journal of Physics: Conference Series, F. IOP Publishing

38. Zhang X, Wu X, He S et al (2021) Precipitation forecast based on CEEMD–LSTM coupled model. Water Supp 21(8):4641–4657

39. Sun X, Zhong K, Han M (2021) A hybrid prognostic strategy with unscented particle filter and optimized multiple kernel relevance vector machine for lithium-ion battery. Measurement 170:108679

40. Lyu Z, Wang G, Gao R (2021) Li-ion battery prognostic and health management through an indirect hybrid model. J Energy Storage 42:102990

41. Meng H, Geng M, Xing J et al (2022) A hybrid method for prognostics of lithium-ion batteries capacity considering regeneration phenomena. Energy 261:125278

42. Zhang S, Zhou J, Wang E et al (2022) State of the art on vibration signal processing towards data-driven gear fault diagnosis. IET collob intell manuf 4(4):249–266

43. Yang K, Wang Y, Li M et al (2023) Modeling topological nature of gas–liquid mixing process inside rectangular channel using RBF-NN combined with CEEMDAN-VMD. Chem Eng Sci 267:118353

44. Qu W, Chen G, Zhang T (2022) An adaptive noise reduction approach for remaining useful life prediction of lithium-ion batteries. Energies 15(19):7422

45. Chen L, Wang H, Chen J et al (2020) A novel remaining useful life prediction framework for lithium-ion battery using grey model and particle filtering. Int J Energy Res 44(9):7435–7449

46. Pang X, Liu X, Jia J et al (2021) A lithium-ion battery remaining useful life prediction method based on the incremental capacity analysis and Gaussian process regression. Microelectron Reliab 127:114405

47. Wang Z, Ta Y, Cai W et al (2023) Research on a remaining useful life prediction method for degradation angle identification two- stage degradation process. Mech Syst Signal Process 184:109747

48. Xu N, Wang X, Meng X et al (2022) Gas concentration prediction based on IWOA-LSTM-CEEMDAN residual correction model. Sensors 22(12):4412

49. Huang S, Zhang J, He Y et al (2022) Short-term load forecasting based on the CEEMDAN-sample entropy-BPNN-transformer. Energies 15(10):3659

50. Torres ME, Colominas MA, Schlotthauer G et al (2011) A com- plete ensemble empirical mode decomposition with adaptive noise; proceedings of the 2011 IEEE international conference on acoustics, speech and signal processing (ICASSP), F. IEEE

51. Arora P, Jalali SMJ, Ahmadian S et al (2022) Probabilistic wind power forecasting using optimised deep auto-regressive recurrent neural networks. IEEE Trans Industr Inform 19(3):2814–2825

52. Zhu S, Yuan X, Xu Z et al (2019) Gaussian mixture model coupled recurrent neural networks for wind speed interval forecast. Energy Convers Manag 198:111772

53. Pei H, Si X-S, Hu C et al (2022) Bayesian deep-learning-based prognostic model for equipment without label data related to life- time. EEE Trans Syst Man Cybern: Systems 53(1):504–517

54. Mokari-Mahallati M, Ebrahimpour R, Bagheri N et al (2023) Deeper neural network models better reflect how humans cope with contrast variation in object recognition. Neurosci Res 192:48–55

55. Li J, Wang Z, Liu X et al (2023) Remaining useful life prediction of rolling bearings using GRU-DeepAR with adaptive failure threshold. Sensors 23(3):1144